



HAL
open science

Organocatalyzed ring-opening polymerization (ROP) of functional beta-lactones: new insights into the ROP mechanism and poly(hydroxyalkanoate)s (PHAs) macromolecular structure

Rama M. Shakaroun, Philippe Jehan, Ali Alaaeddine, Jean-François Carpentier, Sophie M. Guillaume

► To cite this version:

Rama M. Shakaroun, Philippe Jehan, Ali Alaaeddine, Jean-François Carpentier, Sophie M. Guillaume. Organocatalyzed ring-opening polymerization (ROP) of functional beta-lactones: new insights into the ROP mechanism and poly(hydroxyalkanoate)s (PHAs) macromolecular structure. *Polymer Chemistry*, 2020, 11 (15), pp.2640-2652. 10.1039/d0py00125b . hal-02562365

HAL Id: hal-02562365

<https://univ-rennes.hal.science/hal-02562365>

Submitted on 27 May 2020

HAL is a multi-disciplinary open access archive for the deposit and dissemination of scientific research documents, whether they are published or not. The documents may come from teaching and research institutions in France or abroad, or from public or private research centers.

L'archive ouverte pluridisciplinaire **HAL**, est destinée au dépôt et à la diffusion de documents scientifiques de niveau recherche, publiés ou non, émanant des établissements d'enseignement et de recherche français ou étrangers, des laboratoires publics ou privés.

Organocatalyzed ring-opening polymerization (ROP) of functional β -lactones: new insights into the ROP mechanism and poly(hydroxyalkanoate)s (PHAs) macromolecular structure†

Rama M. Shakaroun,^a Philippe Jéhan,^{a,b} Ali Alaeddine,^{*b} Jean-François Carpentier^{*a} and Sophie M. Guillaume^{*a}

^aUniv. Rennes, CNRS, Institut des Sciences Chimiques de Rennes, UMR 6226, F-35042 Rennes, France. E-mail: sophie.guillaume@univ-rennes1.fr, jean-francois.carpentier@univ-rennes1.fr

^bUniv. Libanaise, Campus Universitaire Rafic Hariri Hadath, Faculté des Sciences, Laboratoire de Chimie Médicinale et des Produits Naturels, Beirut, Lebanon. E-mail: Alikassem.alaeddine@ul.edu.lb

^cCentre Régional de Mesures Physiques de l'Ouest-CRMPO, ScanMAT UMS 2001, Université de Rennes 1, France

†Electronic supplementary information (ESI) available: Complementing NMR and MS spectra, SEC traces of the PBPL^{OR}s and kinetics of the polymerizations of BPL^{OR}s. See DOI: 10.1039/d0py00125b

The organocatalyzed ring-opening polymerization (ROP) of various 4-alkoxymethylene- β -propiolactones (BPL^{OR}s; R = CH₂CH=CH₂ (All), CH₂Ph (Bn), (CH₂)₃CH₃ (^tBu), SiMe₂^tBu (TBDMS)) towards the formation of the corresponding poly(hydroxyalkanoate)s (PHAs; poly(BPL^{OR})s (PBPL^{OR}s)) is investigated under mild operating conditions (neat, 60 °C), simply using basic organocatalysts of the guanidine (1,5,7-triazabicyclo [4.4.0]dec-5-ene, TBD), amidine (1,8-diazabicyclo[5.4.0]-undec-7-ene, DBU) or phosphazene (2-*tert*-butylimino-2-diethylamino-1,3-dimethylperhydro-1,3,2-diazaphosphorine, BEMP) type. The polymerization proceeds basically at the same rate as the alike organocatalyzed ROP of related β -lactones (especially the ubiquitous β -butyrolactone (BL) and alkyl β -malolactonates (MLA^Rs)), with BEMP being significantly more active than TBD and DBU. Insights into the polymerization mechanisms are gained through detailed 1D/2D NMR spectroscopy and MALDI-ToF mass spectrometry analyses of the resulting PBPL^{OR}s and in particular through the identification of the nature of the end-capping groups. Each of the three organobases promotes the polymerization in its own way, as dictated by either its basic, nucleophilic or dual behavior.

Introduction

Poly(β -hydroxyalkanoate)s (PHAs) are natural aliphatic polyesters, produced by microorganisms from renewable biomass resources, which accumulate intracellularly in the form of granules and serve as energy storage molecules.¹ Following their first report by Lemoigne in the mid-twenties,² PHAs revealed as valuable biodegradable and biocompatible polyester materials, thereby finding applications as bulk commodity plastics or specialty polymers in various domains such as in agro-food, cosmetic, pharmaceutical or medical industries.³ However, regardless of the length and nature of the alkyl substituent of the side chain at the β -position on their backbone,

bacterial PHAs are isotactic biopolymers, thus limiting their physical, mechanical, and thermal properties, and consequently their range of uses.^{3a,4} To enable more versatility, one can synthetically introduce some functionality on the side chain, to tune, for instance, the solubility, crystallinity, hydrophobicity, degradability, thermal and mechanical properties, in order to meet specific requirements. Ring-opening polymerization (ROP) of the four-membered ring substituted β -lactones is an elected chemical approach to access such well-defined functional PHAs.^{1b,5}

The ROP of various β -lactones, and more commonly of the ubiquitous prototypical β -butyrolactone (BL), has been essentially mediated by metal-based salts⁶ or discrete metal complexes, the latter better enabling the fine control of the molar mass, dispersity, chain-end fidelity, and stereocontrol of the microstructure.⁷ In particular, yttrium complexes stabilized by non-chiral tetradentate diamino or aminoalkoxy bisphenolate ligands efficiently mediate the ROP of (functional) β -lactones,^{7i,j} among which BL,⁸ alkyl β -malolactonates (MLA^Rs),⁹ and more recently, 4-alkoxymethylene- β -propiolactones (BPL^{OR}s)¹⁰ (Fig. 1) and larger 8-membered diolides,¹¹ to give the corresponding PHAs with tuned tacticities (atactic, syndiotactic, isotactic). The -CH₂OR ether groups of BPL^{OR}s and -CO₂R alkoxycarbonyl groups of MLA^Rs, typi-

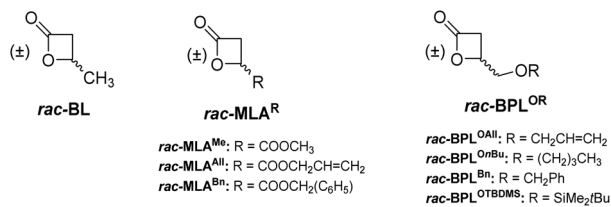


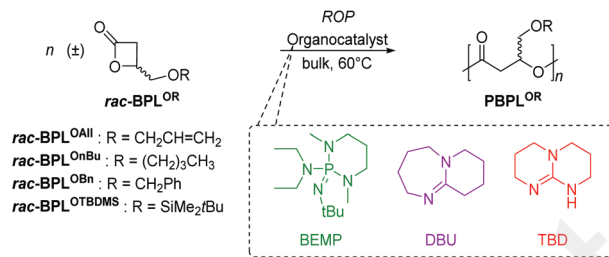
Fig. 1 Substituted β -lactones investigated in ROP towards PHAs, as reported in the literature.

cally range from benzyloxy (OBn; providing an hydrophilic OH segment upon hydrogenolysis), to alkoxy (e.g. OⁿBu, OCH₂CH=CH₂ (Oallyl); providing an hydrophobic chain) (Fig. 1), that can be next exploited in the design of self-assemblies derived from amphiphilic copolymers,¹² or valorized upon exposure to chemical modifications of the highly reactive allyl function.

Apart from metal-based catalyzed ROP, organocatalysis has been more recently revealed as another appealing approach for ROP, especially as a metal-free approach, within the context of polyesters designed for electronics and biomedical applications. Polymerization based on simple organic molecules is thus currently of topical interest for the latter's high chemical stability and long shelf life, low cost, easy availability, ease of handling and high performances.¹³ In fact, within the past two decades, ROP organocatalysts of the most common amine, amidine, guanidine, phosphazene or *N*-heterocyclic carbene (NHC) families, typically 4-(*N,N*-dimethylamino)pyridine (DMAP), 1,8-diazabicyclo[5.4.0]-undec-7-ene (DBU), 1,5,7-triazabicyclo[4.4.0]dec-5-ene (TBD), 2-*tert*-butylimino-2-diethylamino-1,3-dimethylperhydro-1,3,2-diazaphosphorine (BEMP), or 1,3-dimesitylimidazol-2-ylidene (IMes NHC), respectively, have proved most effective toward cyclic esters such as lactide, γ -valerolactone, and ϵ -caprolactone, as pioneered by Hedrick, Waymouth and co-workers.^{13,14} The organocatalyzed ROP of β -lactones is much more challenging because of their reluctance to ring open, in spite of their high ring strain.^{13,15} On the other hand, mechanistic pathways of organocatalyzed ROP are more diverse than those encountered in metal-based ROP. In fact, the polymerization mechanism at play in organocatalyzed ROP strongly depends on the chemical nature of the monomer, catalyst, and/or initiator.¹³

Among the organocatalysts used in ROP, BEMP is effective as a base (^{MeCN}p*K*_a = 27.6)¹⁶ for assorted organic reactions such as Michaël addition and alkylation.¹⁷ Remarkably, TBD is reported as a multifunctional organocatalyst acting as a base (^{MeCN}p*K*_a = 26.0),^{16,18a} proton transfer agent^{18b} or nucleophilic^{18c} catalyst for different types of reaction. DBU, discovered as a super base in the sixties¹⁹ and later identified as a nucleophile,²⁰ recently showed a significant dual activity as a base (^{MeCN}p*K*_a = 24.3)¹⁶ and nucleophile in some organic reactions.²¹ Investigating BEMP, TBD, and DBU in the bulk ROP of β -lactones is thus attractive and challenging.

The first reported attempt to ring-open polymerize BL using the TBD/ROH catalytic system failed at room temperature (in



Scheme 1 Organocatalyzed ROP of $rac-BPL^{OR}$ s towards $PBPL^{OR}$ s.

C₆D₆), whereas increasing the temperature to 50 °C gave oligomers with crotonate byproducts in an uncontrolled reaction.^{14a} Later on, TBD, BEMP and DBU successfully enabled the controlled ROP (neat, no ROH co-initiator, 60 °C) of BL and MLA^{Bn} : PHB (poly(BL)) and $PMLA^{Bn}$ chains apparently α,ω -end-capped with the base and crotonate were thus proposed, as suggested by NMR spectroscopy, SEC and MALDI-ToF MS analyses.²² A proposed mechanism with TBD involved the initial formation of a 1 : 1 organobase-*N*-acylcrotonate intermediate^{14a} and propagation through monomer *O*-acyl cleavage (ESI, Scheme S1†); the ROP promoted by DBU and BEMP, although not deeply investigated, was proposed to proceed similarly. Successful copolymerization of BL and MLA^{Bn} mediated by these same organocatalysts was also achieved.^{12a,23} Yet, a recent reinvestigation of the TBD promoted ROP of BL (neat, 60 °C) by Coulembier and coworkers suggested that carboxylate anions issued from the basic activation of BL by TBD are the actual major active species, while the previously reported *N*-acyl- α,β -unsaturated moiety is a minor growing species. Ultimately, the formation of α -crotonate, ω -carboxylic acid end-capped PHB derived from α -crotonate, ω -COO⁻TBDH⁺ PBL chains, involving an *O*-alkyl cleavage of the monomer, was claimed, as based on studies with a trisubstituted β -lactone, namely *rac*-benzylcarbonyl-3,3-dimethyl-2-oxetanone, and ¹H/DOSY NMR and MALDI-ToF/ESI MS data (Scheme S1†).²⁴

In light of such controversial mechanistic considerations on the ROP of substituted β -lactones, in an effort to gain further information, we herein report on the macromolecular characteristics of the PHAs issued from the organocatalyzed ROP of $rac-BPL^{OR}$ s mediated by BEMP, TBD, or DBU (Scheme 1). Mechanistic pathways at play, specific to each organocatalyst, are proposed from detailed insights provided by 1D/2D NMR spectroscopy and MALDI-ToF MS analyses of the resulting $PBPL^{OR}$ s, and more precisely through the reliable identification of the nature of their end-capping groups.

Experimental section

Methods and materials

All catalytic experiments were performed under an inert argon atmosphere using standard Schlenk line and glovebox techniques. TBD (98%, Aldrich) was used as received. DBU (98%,

Aldrich) and BEMP (>98%, Aldrich) were distilled from CaH₂ prior to use. *Racemic* 4-benzyloxymethyl- β -propiolactone (*rac*-BPL^{OBn}), 4-allyloxymethyl- β -propiolactone (*rac*-BPL^{OAlI}), 4-*n*-butyloxymethyl- β -propiolactone (*rac*-BPL^{OnBu}), and 4-*tert*-butyldimethylsilyloxymethyl- β -propiolactone (*rac*-BPL^{OTBDMS}) were synthesized according to the reported literature procedure, respectively.²⁵ The lactones were dried on CaH₂ and next distilled prior to use.

Instrumentation and measurements

¹H (500 and 400 MHz), ¹³C{¹H} (125 MHz), ³¹P{¹H} (121 MHz) and COSY NMR spectra were recorded on Bruker Avance AM 500 and Ascend 400 spectrometers at 25 °C. ¹H and ¹³C NMR spectra were referenced internally relative to SiMe₄ (δ 0 ppm) using the residual solvent resonances. ³¹P NMR spectra were referenced externally relative to 85% H₃PO₄ (δ 0 ppm).

Number-average molar mass ($\bar{M}_{n,SEC}$) and dispersity ($D_M = \bar{M}_w/\bar{M}_n$) values of the PBPL^{ORs} were determined by size exclusion chromatography (SEC) in THF at 30 °C (flow rate = 1.0 mL min⁻¹) on a Polymer Laboratories PL50 apparatus equipped with a refractive index detector and a set of two ResiPore PLgel 3 μ m MIXED-D 300 \times 7.5 mm columns. The polymer samples were dissolved in THF (2 mg mL⁻¹). All elution curves were calibrated with polystyrene standards; the reported $\bar{M}_{n,SEC}$ values of the PBPL^{ORs} are uncorrected for the difference in hydrodynamic radius vs. polystyrene.

The molar mass of PBPL^{ORs} samples was determined also by ¹H NMR analysis ($\bar{M}_{n,NMR}$) in CDCl₃ from the relative intensities of the signals of the PBPL^{OR} repeating unit methine hydrogen (OCH^c(R)CH₂, δ_{Hc} 5.76–5.19 ppm) and of the crotonate chain-end hydrogen (CH=CH^cC(O), δ_{Hg} 6.99–6.08 ppm).

Monomer conversions were calculated from ¹H NMR spectra of the crude reaction mixtures in CDCl₃ or C₆D₆ by using the integration (Int.) ratio Int._{polymer}/[Int._{polymer} + Int._{monomer}] of the methine hydrogens of each polymer (as stated above) and of each residual monomer (δ 4.63 ppm for BPL^{OBn}, δ 4.65 ppm for BPL^{OAlI}, δ 4.66 ppm for BPL^{OnBu} and δ 4.54 ppm for BPL^{OTBDMS}, in CDCl₃).

Mass spectra were recorded at CRMPO-ScanMAT (Rennes, France). ESI mass spectra were recorded on an orbitrap type Thermo Fisher Scientific Q-Exactive instrument with an ESI source in positive or negative mode by direct introduction at 5–10 μ g mL⁻¹. Samples were prepared in CH₂Cl₂ at 10 μ g mL⁻¹. High resolution MALDI-ToF mass spectra were recorded using an ULTRAFLEX III TOF/TOF spectrometer (Bruker Daltonik GmbH, Bremen, Germany) in positive and/or negative ionization mode. Spectra were recorded using reflectron mode and an accelerating voltage of 25 kV. A mixture of a freshly prepared solution of the polymer in THF or CH₂Cl₂ (HPLC grade, 10 mg mL⁻¹) and DCTB (*trans*-2-(3-(4-*tert*-butylphenyl)-2methyl-2-propenylidene) malononitrile, and a MeOH solution of the cationizing agent (NaI, 10 mg mL⁻¹) were prepared. The solutions were combined in a 1:1:1 v/v/v ratio of matrix-to-sample-to-cationizing agent – if added. The resulting solution (0.25–0.5 mL) was deposited onto the sample target

(Prespotted AnchorChip PAC II 384/96 HCCA) and air or vacuum dried.

General procedure for BPL^{ORs} homopolymerization

In a typical experiment (Table 1, entry 12), in a glovebox, BEMP (10 μ L, 34.6 μ mol) was added using a microsyringe onto BPL^{OBn} (0.28 g, 1.475 mmol, 42 equiv.) placed in a Schlenk flask. The neat reaction mixture was then stirred in an oil bath at 60 °C over the appropriate reaction time (reaction times were not systematically optimized). The polymerization was quenched by addition of an excess of undried CH₂Cl₂ (1 mL). The resulting mixture was concentrated to dryness under vacuum and the conversion was determined by ¹H NMR analysis of the residue dissolved in CDCl₃ or C₆D₆. The crude residue was then dissolved in CH₂Cl₂ (1 mL) and precipitated in cold pentane (10 mL, 0 °C) (repeated twice, thus enabling the removal of potential unreacted/free base), filtered and dried overnight at 60 °C using a vacuum oven. All recovered polymers were then analyzed by NMR, MALDI-ToF and ESI MS, and SEC (refer to ESI[†]). PBL^{OR} samples were stored under inert atmosphere at 0 °C.

Results and discussion

The organocatalyzed ROP of *rac*-BPL^{ORs} has been investigated using BEMP, TBD or DBU, under neat conditions (solvent-free), at 23–60 °C, in the absence of an alcohol as co-initiator. These operating conditions were the same as those previously implemented in the successful alike ROP of BL and MLA^{Bn}.^{22,26} Representative results of these ROP experiments are gathered in Tables 1–3. Insights into the chemical structure of the resulting PBPL^{ORs} were gained from detailed NMR spectroscopy and MS investigations. Close examination of the nature of the chain-end groups then supported different operating modes for each organocatalyst.

General characteristics of the ROP of *rac*-BPL^{ORs} mediated by BEMP, TBD or DBU

The neat ROP of *rac*-BPL^{ORs} has been first investigated using BEMP as catalyst. While effective at room temperature, the polymerization was found, as expected, to proceed faster at higher temperatures (40 or 60 °C; Table 1). Subsequent ROP experiments of BPL^{ORs} were thus all performed at 60 °C (Tables 1–3).

The nature of the ether moiety of the CH₂OR group appeared to similarly influence the rate of the polymerization from one organocatalyst to another, as revealed by kinetic monitoring by ¹H NMR spectroscopy of the ROP of *rac*-BPL^{ORs} (Fig. 2). Using BEMP, TBD or DBU, while BPL^{OBn} exhibited a slightly faster rate of polymerization than BPL^{OnBu}, both monomers polymerized less rapidly than BPL^{OAlI}, but much faster than BPL^{OTBDMS} (Fig. 2, Tables 1–3). Regardless of the ether moiety, the BPL^{ORs} polymerized significantly more slowly (typical turnover frequency (TOF) < 15 h⁻¹) than β -butyrolactone and alkyl β -malolactonates MLA^Rs (typical

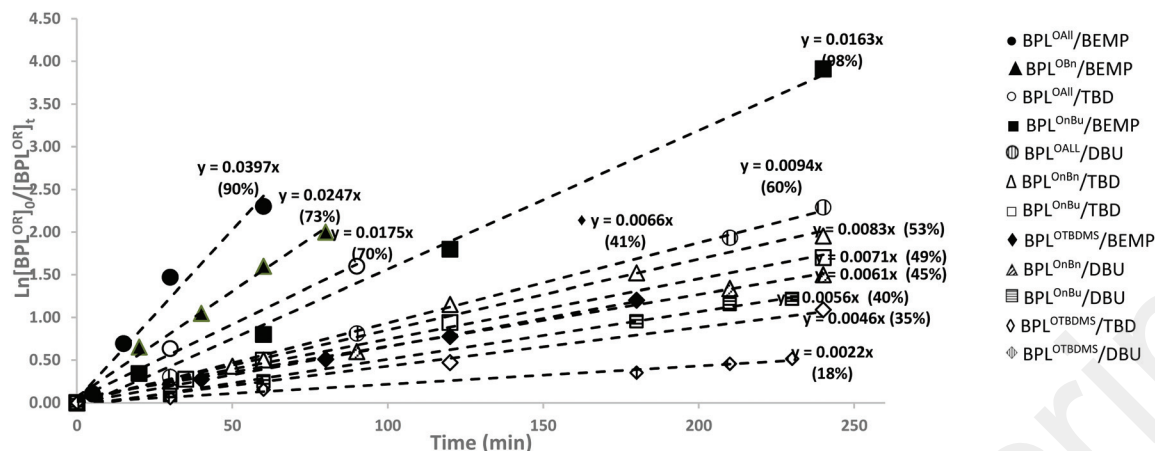


Fig. 2 Logarithmic plot of the kinetics of the ROP of *rac*-BPL^{OR}s (40 equiv.) mediated by BEMP (1 equiv.) (Table 1, entries 3, 6, 12 and 15), TBD (Table 2, entries 1, 4, 7 and 8) and DBU (Table 3, entries 1–4), at 60 °C in bulk; the data in parentheses are the final monomer conversions (before reaching a high viscosity and diffusion limits).

TOF = 100 h⁻¹, and 150 h⁻¹, respectively) under the same conditions.²² BEMP proved significantly more active than TBD and DBU, a general trend also reported for the alike ROP of BL and MLA^{Bn}.²² Also, the organocatalysts herein investigated revealed less efficient than the yttrium-based catalyst which typically afforded the corresponding PBPL^{OR}s with quantitative yields within 2 h at 23 °C (TOF = *ca.* 25 h⁻¹).^{10a} Note that, in contrast to syndio- and isotactic polymers produced by bisphenolate yttrium catalysts,¹⁰ all PBPL^{OBn}s recovered from the three organocatalysts revealed atactic, as evidenced by the ¹³C {¹H} NMR spectra (ESI, Fig. S1†).

The molar masses were evaluated by ¹H NMR analysis ($\bar{M}_{n,NMR}$) from the relative intensities of the signals of the PBPL^{OR} main-chain methine hydrogen and of the crotonate

chain-end (*vide infra*) hydrogens (refer to the Experimental section). These values generally increased proportionally to the monomer loading and remained in fair agreement with the molar mass values calculated from the monomer conversion ($\bar{M}_{n,theo}$; not taking into account end-capping groups). The number-average molar mass values as determined by SEC ($\bar{M}_{n,SEC}$) were also generally in fair agreement with the $\bar{M}_{n,NMR}$ data. The dispersities (D_M), in the range 1.09–1.53 (ESI, Fig. S2†), most likely evidenced the occurring, yet with a limited extent, of undesirable intra- and intermolecular transesterification reactions (backbiting and reshuffling, respectively) or other transfer reactions (*vide infra*), or possibly a rate of initiation competitive with that of propagation. The control in terms of molar mass and limited side reactions, and the catalytic activity

Table 1 Characteristics of the PBPL^{OR}s synthesized by ROP of *rac*-BPL^{OR}s mediated by BEMP^a

Entry	BPL ^{OR}	$[BPL^{OR}]_0/[BEMP]_0$	Temp. (°C)	Reaction time ^b (h)	Conv. ^c (%)	$\bar{M}_{n,theo}$ ^d (g mol ⁻¹)	$\bar{M}_{n,NMR}$ ^e (g mol ⁻¹)	$\bar{M}_{n,SEC}$ ^f (g mol ⁻¹)	D_M ^f
1	BPL ^{OAll}	40	25	21	91	5150	4100	4600	1.09
2	BPL ^{OAll}	40	40	7	50	2850	1800	1300	1.17
3	BPL ^{OAll}	40	60	3	97	5500	4800	3900	1.26
4	BPL ^{OnBu}	40	25	19	72	4550	4850	6200	1.18
5	BPL ^{OnBu}	44	40	8	78	5400	5650	7700	1.16
6	BPL ^{OnBu}	40	60	4	98	6200	3800	4900	1.32
7	BPL ^{OBn}	43	25	12	60	4950	3300	2800	1.53
8	BPL ^{OBn}	15	40	3	94	2700	3100	2500	1.32
9	BPL ^{OBn}	40	40	9	84	6450	5500	5000	1.15
10	BPL ^{OBn}	60	40	10	32	3700	1700	1500	1.38
11	BPL ^{OBn}	15	60	4	100	2900	2500	2400	1.21
12	BPL ^{OBn}	40	60	3	82	6300	4200	3100	1.27
13	BPL ^{OBn}	60	60	2	50	5750	3000	2800	1.53
14	BPL ^{OTBDMS}	40	40	6	34	2950	2000	1900	1.20
15	BPL ^{OTBDMS}	35	60	8	88	6650	3600	3300	1.18

^a Results are representative of at least duplicated experiments performed neat. ^b The reaction time was not necessarily optimized. ^c BPL^{OR} conversion as determined by ¹H NMR analysis of the crude reaction mixture (refer to the Experimental section). ^d Theoretical molar mass calculated from the relation: $[BPL^{OR}]_0/[BEMP]_0 \times \text{Conv.}_{BPL^{OR}} \times M_{BPL^{OR}}$, *i.e.* without considering end-capping groups, with $M_{BPL^{OAll}} = 142$ g mol⁻¹, $M_{BPL^{OnBu}} = 158$ g mol⁻¹, $M_{BPL^{OBn}} = 192$ g mol⁻¹, and $M_{BPL^{OTBDMS}} = 216$ g mol⁻¹. ^e Experimental molar mass value determined by ¹H NMR analysis of the isolated polymer, from the resonances of the crotonate end-group (refer to the Experimental section). ^f Experimental molar mass and dispersity values as determined by SEC in THF using a RI detector at 30 °C vs. polystyrene standards.

Table 2 Characteristics of the PBPL^{OR}s synthesized by ROP of *rac*-BPL^{OR}s mediated by TBD^a

Entry	BPL ^{OR}	[BPL ^{OR}] ₀ /[TBD] ₀	Temp. (°C)	Reaction time ^b (h)	Conv. ^c (%)	$\bar{M}_{n,theo}$ ^d (g mol ⁻¹)	$\bar{M}_{n,NMR}$ ^e (g mol ⁻¹)	$\bar{M}_{n,SEC}$ ^f (g mol ⁻¹)	D_M ^f
1	BPL ^{OAll}	43	60	4	81	4950	3600	3100	1.41
2	BPL ^{OnBu}	40	25	19	21	1350	1000	1000	1.14
3	BPL ^{OnBu}	42	40	9	44	2900	2800	2100	1.14
4	BPL ^{OnBu}	40	60	7	68	4300	3300	3200	1.29
5	BPL ^{OnBu}	75	60	16	88	10 450	11 850	7000	1.15
6	BPL ^{OBn}	20	60	3	61	2350	2100	1100	1.26
7	BPL ^{OBn}	41	60	6	70	5500	4300	3900	1.32
8	BPL ^{OTBDMS}	40	60	8	40	3450	1000	1100	1.34

^a Results are representative of at least duplicated experiments performed neat. ^b The reaction time was not necessarily optimized. ^c BPL^{OR} conversion as determined by ¹H NMR analysis of the crude reaction mixture (refer to the Experimental section). ^d Theoretical molar mass calculated from the relation: [BPL^{OR}]₀/[TBD]₀ × Conv._{BPLOR} × M_{BPLOR} , *i.e.* without considering end-capping groups, with $M_{BPL^{OAll}}$ = 142 g mol⁻¹, $M_{BPL^{OnBu}}$ = 158 g mol⁻¹, $M_{BPL^{OBn}}$ = 192 g mol⁻¹, and $M_{BPL^{OTBDMS}}$ = 216 g mol⁻¹. ^e Experimental molar mass value as determined by ¹H NMR analysis of the isolated polymer, from the resonances of the crotonate end-group (refer to the Experimental section). ^f Experimental molar mass and dispersity values as determined by SEC in THF using a RI detector at 30 °C vs. polystyrene standards.

Table 3 Characteristics of the PBPL^{OR}s synthesized by ROP of *rac*-BPL^{OR}s mediated by DBU^a

Entry	BPL ^{OR}	[BPL ^{OR}] ₀ /[DBU] ₀	Reaction time ^b (h)	Conv. ^c (%)	$\bar{M}_{n,theo}$ ^d (g mol ⁻¹)	$\bar{M}_{n,NMR}$ ^e (g mol ⁻¹)	$\bar{M}_{n,SEC}$ ^f (g mol ⁻¹)	D_M ^f
1	BPL ^{OAll}	40	8	58	3300	1700	1300	1.18
2	BPL ^{OnBu}	40	10	70	4400	2500	2500	1.30
3	BPL ^{OBn}	50	5	51	4900	1650	1500	1.29
4	BPL ^{OTBDMS}	40	8	25	2200	2600	1800	1.12

^a Results are representative of at least duplicated experiments performed neat at 60 °C. ^b The reaction time was not necessarily optimized. ^c BPL^{OR} conversion as determined by ¹H NMR analysis of the crude reaction mixture (refer to the Experimental section). ^d Theoretical molar mass calculated from the relation: [BPL^{OR}]₀/[DBU]₀ × Conv._{BPLOR} × M_{BPLOR} , *i.e.* without considering end-capping groups, with $M_{BPL^{OAll}}$ = 142 g mol⁻¹, $M_{BPL^{OnBu}}$ = 158 g mol⁻¹, $M_{BPL^{OBn}}$ = 192 g mol⁻¹, and $M_{BPL^{OTBDMS}}$ = 216 g mol⁻¹. ^e Experimental molar mass value as determined by ¹H NMR analysis of the isolated polymer, from the resonances of the crotonate end-group (refer to the Experimental section). ^f Experimental molar mass and dispersity values as determined by SEC in THF using a RI detector at 30 °C vs. polystyrene standards.

and productivity, were not optimized, since the focus of the present work was placed on the mechanism at play.

NMR, MALDI-ToF and ESI MS of the PBPL^{OR}s and mechanistic insights into the ROP of *rac*-BPL^{OR}s mediated by BEMP, TBD or DBU

All the purified (reprecipitated twice – refer to the Experimental section) PBPL^{OR}s samples isolated from the ROP of *rac*-BPL^{OR}s mediated by BEMP, TBD or DBU were characterized by ¹H, J-MOD and 2D (COSY) NMR spectroscopy and MALDI-ToF and ESI MS (refer to ESI[†]). These analyses enabled to probe the nature of the end-capping groups of the PHAs and therefrom to suggest the possible corresponding ROP mechanism specific to each organocatalyst.

PBPL^{OR}s recovered from the ROP of *rac*-BPL^{OR}s mediated by BEMP

The typical ¹H and J-MOD NMR spectra of PBPL^{ORn}s recovered from the ROP of *rac*-BPL^{OR}s mediated by BEMP (Table 1, Fig. S3–S5[†]) are depicted in Fig. 3 with PBPL^{OBn}. Regardless of the monomer/polymer ether substituent (OBn, OAll, OⁿBu, OTBDMS), besides the main chain repeating unit typical methine and methylene backbone hydrogens' signals (δ_{1H} ppm 5.39 (OCH^cCH₂) and 2.67 (CH₂^{a,b}C(O))), resonances for both crotonate (δ_{1H} ppm 6.99 (CHⁱ=CHCH₂O), 6.14 (CH=CH^gC(O)

O)) and BEMP (especially methyl signals: δ_{1H} ppm 1.36 (NC(CH^h)₃) and 1.15 (NCH₂CH^k) moieties were clearly observed. The corresponding carbon signals of these two moieties were assigned from the J-MOD spectrum (Fig. 3). All signals' assignments were supported by 2D COSY NMR analyses; the correlation between the vinylic hydrogens and the end-group methylene hydrogens supports a crotonate chain-end (ESI, Fig. S6–S10[†]). ¹H NMR monitoring of the α,β -unsaturation-to-BEMP molar ratio revealed an increase of the crotonate group content during the course of the reaction and/or at a higher temperature (60 °C) and/or at a larger initial monomer loading (40 vs. 60 equiv.) (Table 1, entries 9, 10, 12 and 13; ESI, Fig. S11[†]), in agreement with the suggested mechanism (Scheme 2, *vide infra*). Closer examination of the ¹H NMR signals of the BEMP moiety, and as further corroborated by ³¹P NMR analysis, showed that the resonances correspond to the protonated base [BEMPH]⁺; this was demonstrated by the significant shift of the NC(CH^h)₃ ¹H ($\Delta\delta$ -0.25 ppm) and ³¹P ($\Delta\delta$ 27.18 ppm) resonances, relative to the free BEMP signals, respectively, and by the comparison with a genuine sample of [BEMPH]⁺[OAc]⁻ (ESI, Fig. S12[†]). Hence, BEMP is present in its protonated form [BEMPH]⁺ during the polymerization process, excluding the possibility of it behaving as a nucleophile that would ring open the monomer *via* an *O*-acyl cleavage.

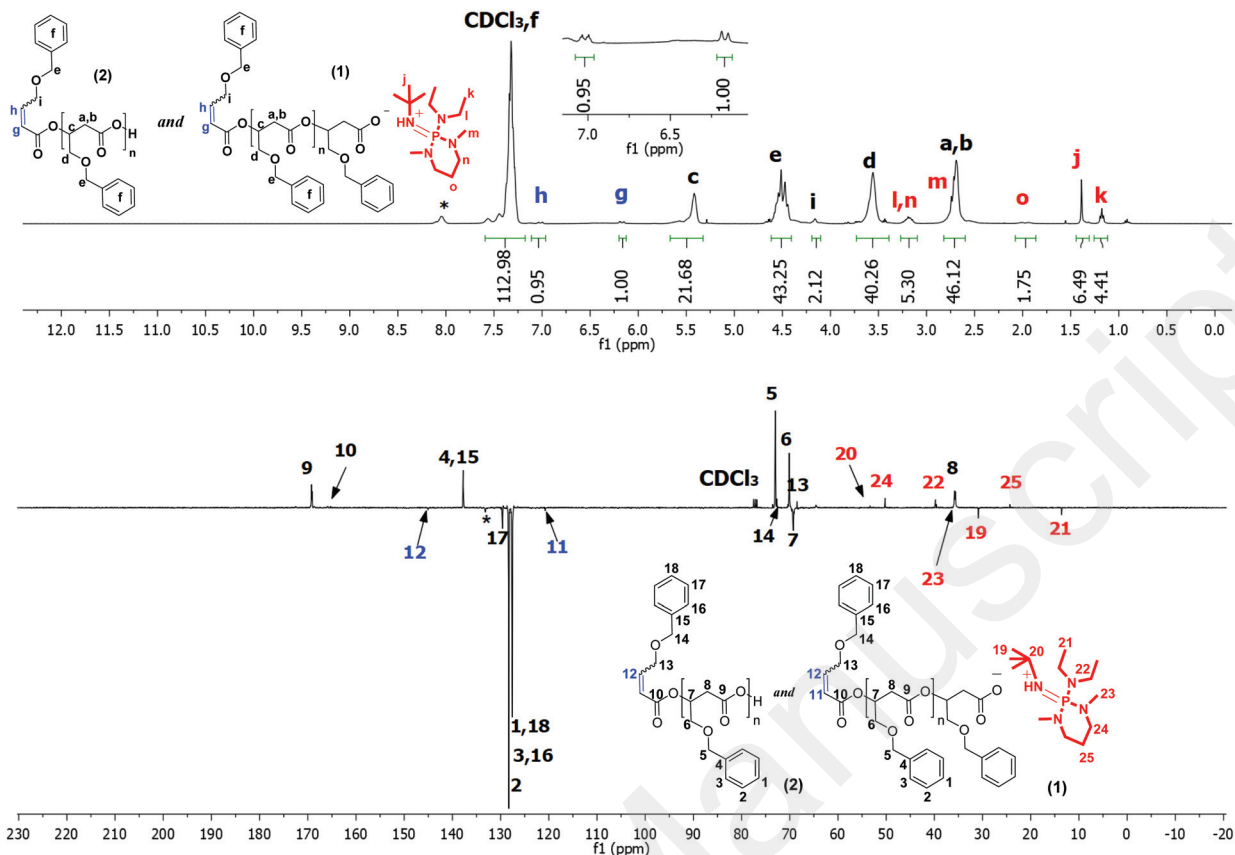
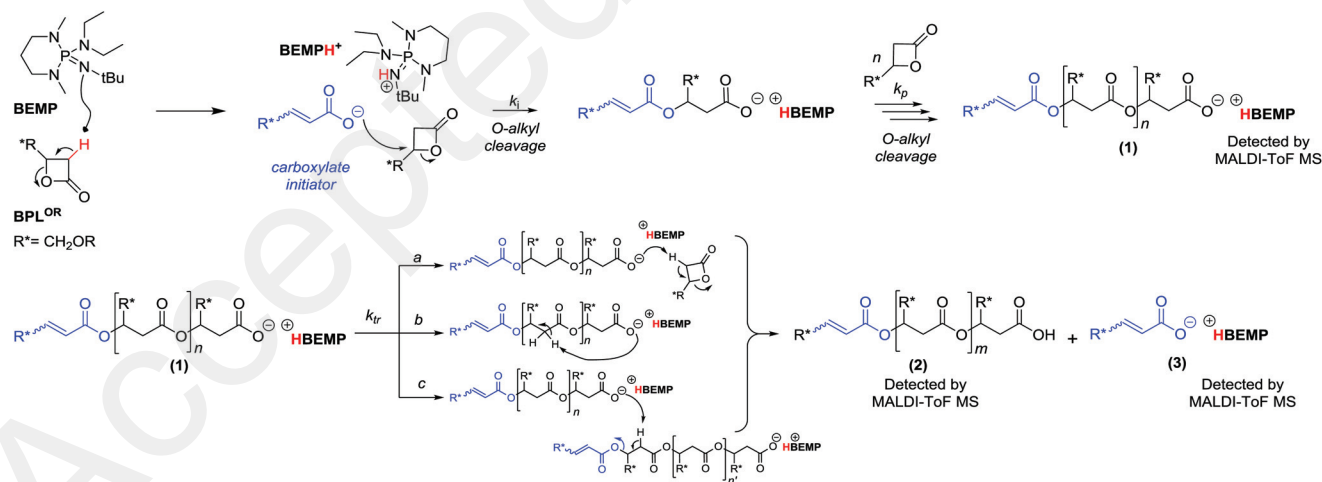


Fig. 3 ^1H (500 MHz, CDCl_3 , 25 °C) (top) and J-MOD (125 MHz, CDCl_3 , 25 °C) (bottom) NMR spectra of PBPL^{OBn} with $[\text{BnOCH}_2\text{CH}=\text{CHCOO}(\text{PBL}^{\text{OBn}})]^-[\text{BEMPH}]^+$ (Scheme 2, 1) and $\text{BnOCH}_2\text{CH}=\text{CHCOO}(\text{PBL}^{\text{OBn}})\text{H}$ (Scheme 2, 2) (note that the possible $[\text{BnOCH}_2\text{CH}=\text{CHCOO}]^-[\text{BEMPH}]^+$ species (Scheme 2, 3) is not depicted) recovered from the ROP of $\text{rac-BPL}^{\text{OBn}}$ mediated by BEMP (Table 1, entry 12) (*: unidentified minor impurity not observed in other spectra of PBPL^{OR} obtained from BEMP (ESI, Fig. S3–S7†)).



Scheme 2 Proposed mechanism for the ROP of $\text{rac-BPL}^{\text{ORs}}$ mediated by BEMP proceeding *via* a proton transfer reaction to generate *in situ* the carboxylate initiating moiety (k_i , k_p , k_{tr} , refer to the rate constant of initiation, propagation, and transfer reactions, respectively), showing the various macromolecular species (1–3).

The MALDI-ToF (Fig. 4) and ESI (ESI, Fig. S13†) mass spectra of PBPL^{OBn} samples prepared by the BEMP-mediated ROP are both consistent with the above-mentioned

α -crotonate, ω -carboxylic acid terminated polymer. Indeed, the spectra showed a major population of PBPL^{OBn} with a repeating unit of 192 g mol^{-1} end-capped with a benzyloxycrotonate

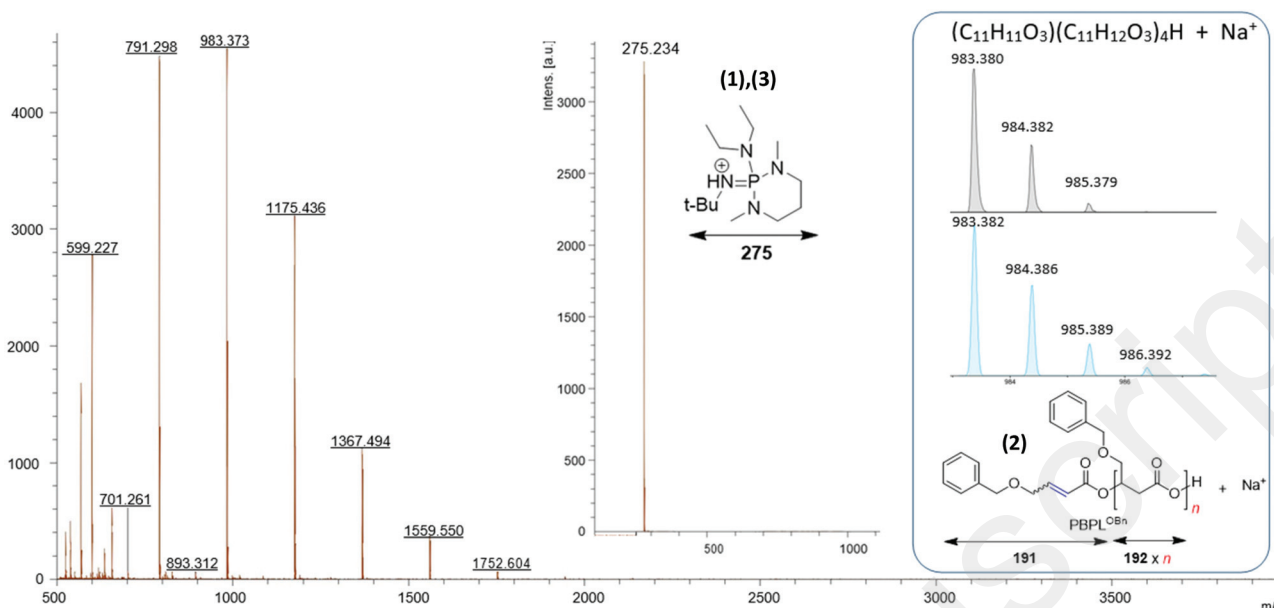


Fig. 4 MALDI-ToF mass spectrum (positive mode, DCTB matrix, Na⁺ cationizing salt) of a sample freshly synthesized from the ROP of *rac*-BPL^{OBn} mediated by BEMP (Table 1, entry 11) showing populations corresponding to PBPL^{OBn} macromolecules end-capped with both an α -crotonate and an ω -carboxylic acid end-groups (Scheme 2, **2**; the right zoomed regions correspond to the simulated (blue, bottom) and experimental (black, top) spectra), and to [BEMPH]⁺ (Scheme 2, **1,3**; the top middle zoomed region shows the [BEMPH]⁺ fragment recorded).

and a carboxylic acid groups (the latter which was not observed in the ¹H, ¹³C or HMBC NMR spectra; ESI, Fig. S1, S10[†]), as unequivocally supported by the close match of the simulated isotopic distribution with *e.g.* $m/z_{\text{exp}} = 983.380 \text{ g mol}^{-1}$ vs. $m/z_{\text{simul}} = 983.382 \text{ g mol}^{-1}$ for $n = 4$ (see right zoomed region). [BEMPH]⁺ was also clearly observed at $m/z_{\text{exp}} = 275.234 \text{ g mol}^{-1}$ (middle zoomed region) vs. $m/z_{\text{simul}} = 275.236 \text{ g mol}^{-1}$. However, its counter anion, the carboxylate (macro)molecule(s) (Scheme 2-1,3) could not be observed under the positive MALDI-ToF MS conditions while analysis under the negative mode did not revealed sensitive enough. No cyclic polymer therein was observed.²⁷

Considering these spectroscopic and spectrometric evidences of the formation of a mixture of α -benzyloxy crotonate, ω -COOH PBPL^{OBn} and [BEMPH]⁺, we may propose the ROP mechanism depicted in Scheme 2. Thus, BEMP would act as a basic pre-initiator that abstracts one of the methylene hydrogen in α -position of the BPL^{OR} monomer, thereby generating an α,β -unsaturated carboxylate species as the real initiator, which in turn would propagate the polymerization *via* *O*-alkyl cleavage of further incoming monomer units. Carboxylate initiators have previously been reported to promote the ROP of BL and MLA^{Bn} through such *O*-alkyl opening, a behavior specific to β -lactones.^{5,28} Ultimately, (ROCH₂CH=CHC(O)O)–PBPL^{OBn}–H chains would form upon termination/transfer reactions. Transfer reactions may (a) involve the monomer ($k_{\text{tr,a}}$), (b) take place intramolecularly ($k_{\text{tr,b}}$), and/or (c) intermolecularly ($k_{\text{tr,c}}$), eventually generating a shorter active macromolecular chain ready to propagate (similar to **1**), a dormant chain with a carboxylic acid end-group (**2**), and/or the carboxylate initiator [BnOCH₂CH=CHC

(O)O]–[BEMPH]⁺ (**3**). Such side-reactions could, besides a possible slow initiation, account for the slight discrepancies between experimental molar mass values ($\bar{M}_{n,\text{SEC}}$, $\bar{M}_{n,\text{NMR}}$) and $\bar{M}_{n,\text{theo}}$ as well as for the slightly broad dispersities.²⁹ Reinterpretation of the previously reported MALDI-ToF mass spectra of PHB and PMLA^{Bn}, similarly synthesized by ROP of *rac*-BL and MLA^{Bn}, respectively, mediated by BEMP (ESI, Fig. S14 and S15[†]),²² further supports this suggested mechanism.

PBPL^{OR}s recovered from the ROP of *rac*-BPL^{OR}s mediated by TBD

The typical ¹H, 2D and J-MOD NMR spectra of PBPL^{OR}s recovered from the ROP of *rac*-BPL^{OR}s mediated by TBD (Table 2) are exemplified in Fig. 5 with PBPL^{OBn} and in ESI, Fig. S16–S19,† with PBPL^{OR}s. All these NMR spectra unambiguously showed, alongside the characteristic backbone methine and methylene hydrogens' signals, the resonances of both crotonate and TBD moieties (δ_{H} ppm 3.28 (CH₂N=C(N)NHCH^o₂), 3.20 (CH₂N(C)CH^m₂), and 1.93 (CH₂CH^{k,n}₂CH₂)). The 2D COSY NMR spectra evidenced, similarly as with BEMP, a correlation between the vinylic and methylene hydrogens of the crotonate end-group, supporting the crotonate chain-end (ESI, Fig. S18 and S19[†]).

Further information was gained from MALDI-ToF MS analyses of the isolated PBPL^{OR} samples (Fig. 6). Two distinct populations of macromolecules were observed with a repeating unit of 192 g mol⁻¹. A first population **I** corresponds to PBPL^{OBn} flanked with a TBD-*N*-acyl- α,β -unsaturated species and hydroxy chain-ends (Scheme 3, **6**), as unequivocally confirmed by the isotopic simulation (*e.g.* $m/z_{\text{exp}} = 1659.753 \text{ g mol}^{-1}$ vs.

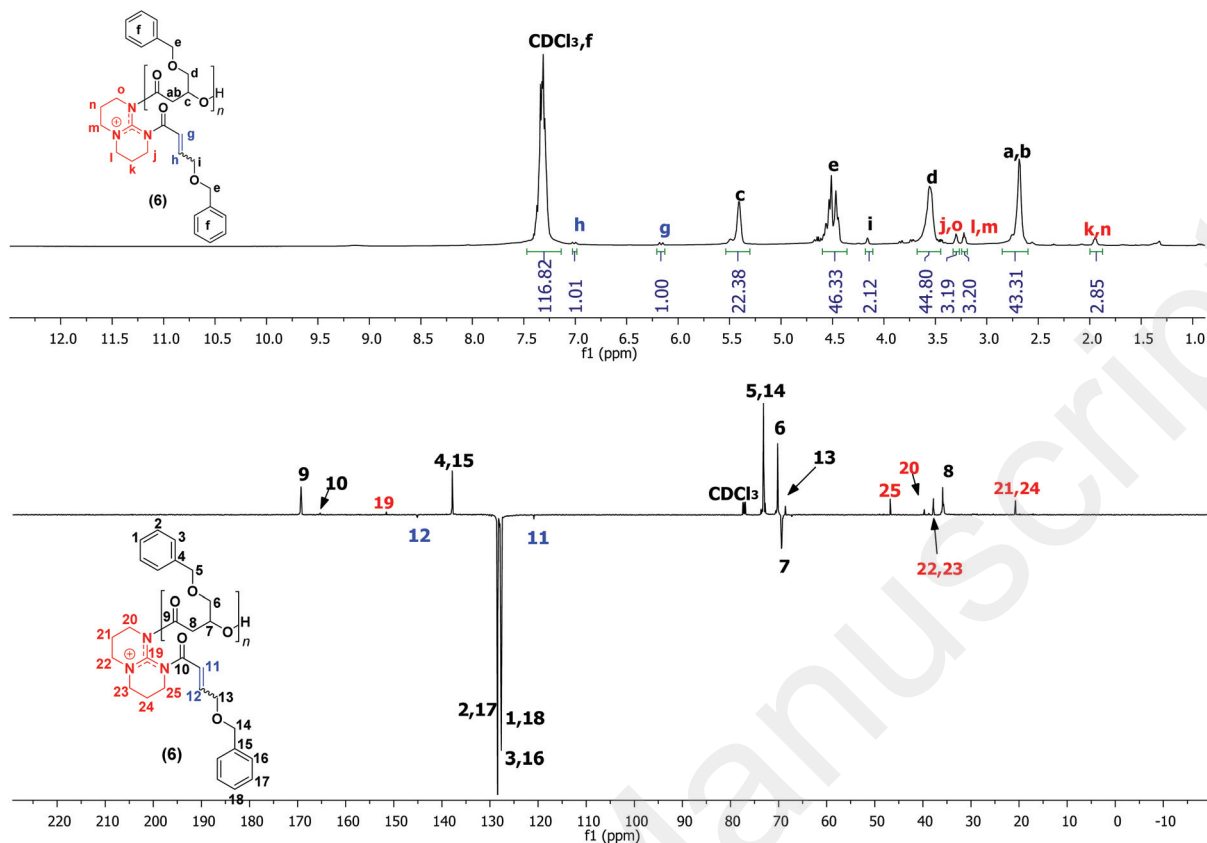


Fig. 5 ^1H (500 MHz, CDCl_3 , 25 $^\circ\text{C}$) (top) and J-MOD (125 MHz, CDCl_3 , 25 $^\circ\text{C}$) (bottom) NMR spectra of a purified PBPL^{OBn} sample recovered from the ROP of $\text{rac-BPL}^{\text{OBn}}$ mediated by TBD (Table 2, entry 7), depicting only one (I, Scheme 3, 6) out of the two populations (I and II, Scheme 3, 6, 8) observed by MALDI-ToF MS (Fig. 6).

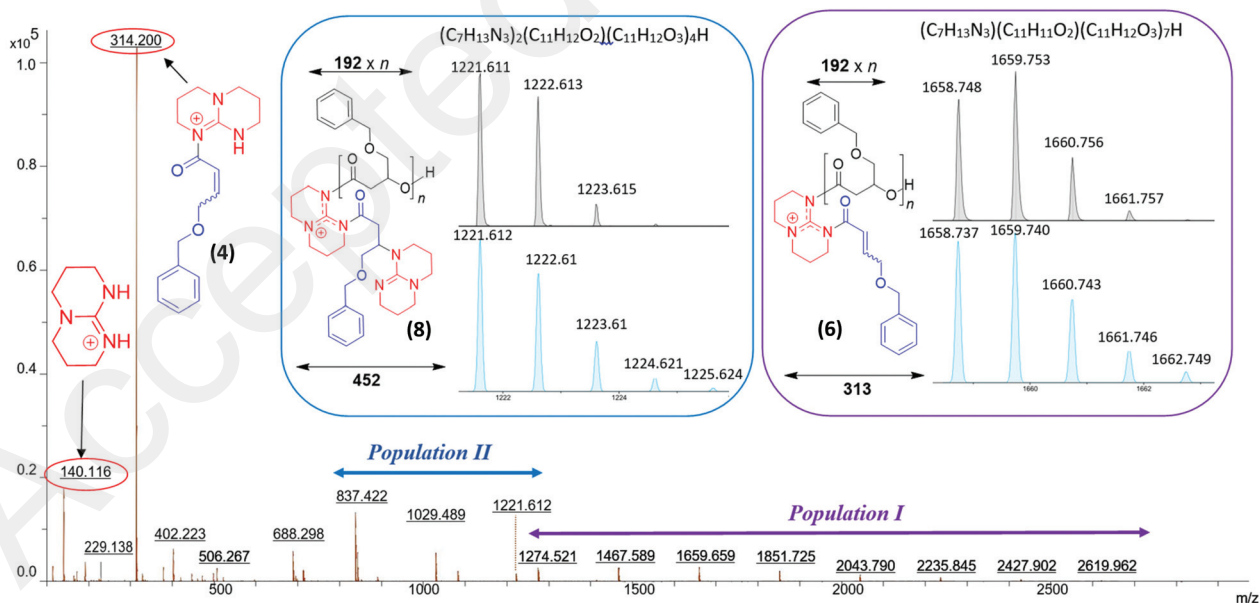
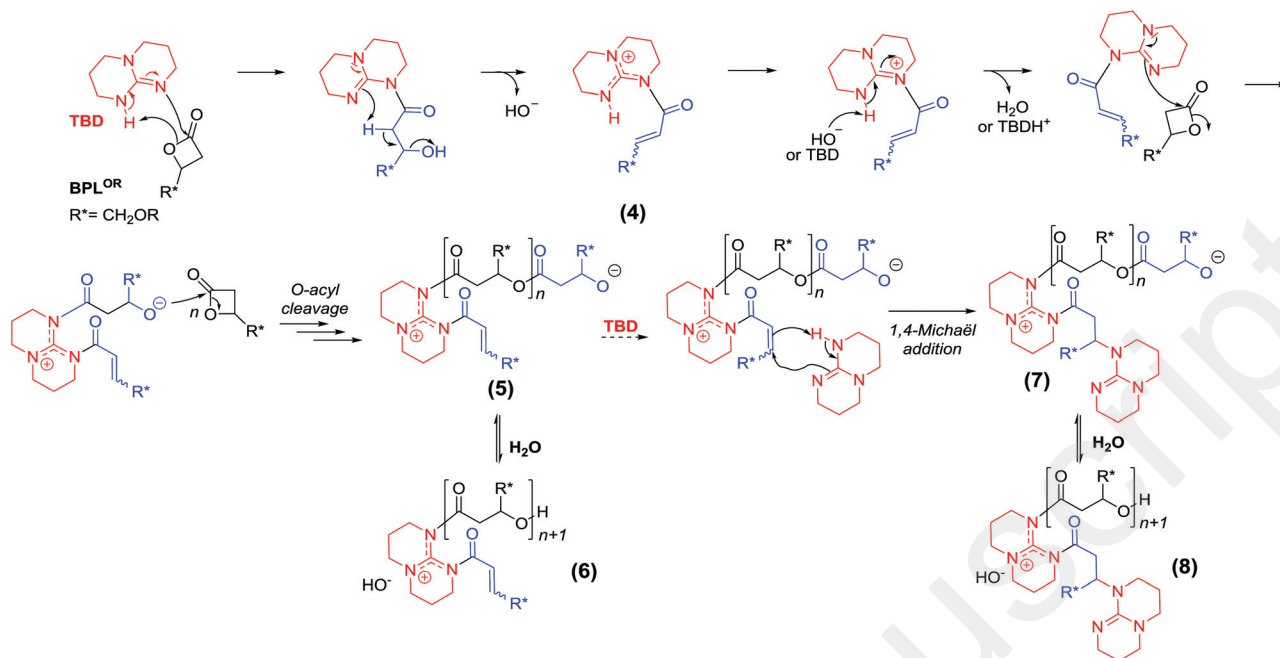


Fig. 6 MALDI-ToF mass spectrum (positive mode, DCTB matrix, Na^+ cationizing salt) of a sample freshly synthesized from the ROP of $\text{rac-BPL}^{\text{OBn}}$ mediated by TBD (Table 2, entry 6) showing populations corresponding to PBPL^{OBn} macromolecules end-capped with both an α -benzyloxycrotonate-TBD and an ω -hydroxy end-groups (population I; Scheme 3, 6), and to a subsequently modified population I where a TBD molecule is added onto the crotonate moiety to give population II (Scheme 3, 8); the zoomed regions correspond to the simulated (blue, bottom) and experimental (black, top) corresponding spectra, respectively. Species TBD : BPL^{OR} (Scheme 3, 4) and $[\text{TBDH}]^+$ are also observed.



Scheme 3 Proposed mechanism for the ROP of *rac*-BPL^{OR}s mediated by TBD, proceeding via an *O*-acyl cleavage of BPL^{OR} into species 5 mediated by 4, and/or the plausible side polymer species 7. Species 6 and 8 refer to the protonated form of 5 and 7, respectively, showing the various (macro) molecular species (4–8).

$m/z_{\text{simul}} = 1659.740 \text{ g mol}^{-1}$ for $n = 7$; see right zoomed region (purple)). This TBD-*N*-acyl- α,β -unsaturated species most likely originates from the 1:1 TBD:BPL^{OR} adduct (Scheme 3, 4) from which H₂O or [TBDH]⁺ is then eliminated. This is reminiscent of the mechanism initially suggested for the ROP of BL and MLA^{Bn} mediated by this same guanidine.²² This adduct would propagate the polymerization via an *O*-acyl cleavage operated by the second nucleophilic nitrogen of TBD, generating a zwitterionic propagating species (Scheme 3, 5) ultimately giving population I (Fig. 6, Scheme 3, 6) after protonation.^{30a} The second population II, issued from the former one, features an additional TBD moiety, as supported by the isotopic simulation with e.g. $m/z_{\text{exp}} = 1221.611 \text{ g mol}^{-1}$ vs. $m/z_{\text{simul}} = 1221.612 \text{ g mol}^{-1}$ for $n = 4$ (see left zoomed region (blue)). Most likely, the α,β -unsaturation from 5 acts as a Michael acceptor towards TBD, thereby generating macromolecules 7 which form population II (Fig. 6, Scheme 3, 8) upon protonation.^{30b} From these two populations, [TBDH]⁺ ($m/z_{\text{exp}} = 140.116 \text{ g mol}^{-1}$) and TBD-crotonate⁺ ($m/z_{\text{exp}} = 314.200 \text{ g mol}^{-1}$) species could be abstracted, as observed in the experimental mass spectrum (Fig. 6). From these results, it thus appears that TBD would be following a nucleophilic pathway to ring-open BPL^{OR}s, rather than a basic one, as depicted in Scheme 3. This is reminiscent of the mechanism reported for the ROP of ϵ -caprolactone promoted by TBD under similar bulk operating conditions.³¹ Further support of this mechanism was gained from the re-interpretation of the previously reported MALDI-ToF mass spectra of PHB and PMLA^{Bn} similarly obtained by ROP of *rac*-BL and MLA^{Bn} mediated by TBD (ESI, Fig. S20 and S22[†]), in agreement with the corresponding

NMR spectra (Fig. S21 and S23[†]).²² On the other hand, this is in contrast with the TBD-mediated anionic ROP of BL reported recently by Coulembier and co-workers in which TBD is proposed to activate the β -lactone via its basic character.²⁴

PBPL^{OR}s recovered from the ROP of *rac*-BPL^{OR}s mediated by DBU

Similarly to the PBPL^{OR}s synthesized using BEMP or TBD, 1D and 2D ¹H NMR analyses of PBPL^{OR}s prepared from the alike ROP of *rac*-BPL^{OR}s mediated by DBU unambiguously evidenced the presence of both α,β -unsaturation and DBU moieties (δ_{H} ppm 3.37 (CH^{*i*}₂N(C)CH^{*k*}₂), 3.34 (CNCH^{*m*}₂CH₂), 2.80 (CH₂CH^{*n*}₂C(N)=N), 1.93 (NCH₂CH^{*q*}₂CH₂), 1.70 (CH₂CH₂CH^{*p*}₂CH^{*o*}₂CH₂), 1.61 (CH₂CH^{*q*}₂CH₂CH₂CH₂) (Fig. 7, top) for PBPL^{OBn}, and ESI, Fig. S24 and S25[†] for other PBPL^{OR}s). The corresponding carbon resonances and 2D correlations were identified in the J-MOD and COSY spectra, respectively (Fig. 7, bottom for PBPL^{OBn}, and ESI, Fig. S24–S27[†] for other PBPL^{OR}s).

MALDI-ToF MS of the thus prepared PBPL^{OR}s provided valuable information. Two macromolecular populations with a repeating unit of 192 g mol⁻¹ are clearly observed in the mass spectrum of PBPL^{OBn} (Fig. 8). The first population I is consistent with PBPL^{OBn} chains end-capped with a β -hydroxyester and DBU moieties (e.g. $m/z_{\text{exp}} = 1113.526 \text{ g mol}^{-1}$ vs. $m/z_{\text{simul}} = 1113.532 \text{ g mol}^{-1}$ for $n = 5$) in agreement with the simulated isotopic spectrum (see left zoomed region (blue)). The other population II features a benzyloxy-crotonate and a carboxylic acid chain-end-groups, matching the isotopic simulation, with e.g. $m/z_{\text{exp}} = 2328.869 \text{ g mol}^{-1}$ vs. $m/z_{\text{simul}} = 2328.936 \text{ g mol}^{-1}$ for $n = 11$ (see right zoomed region (purple)).

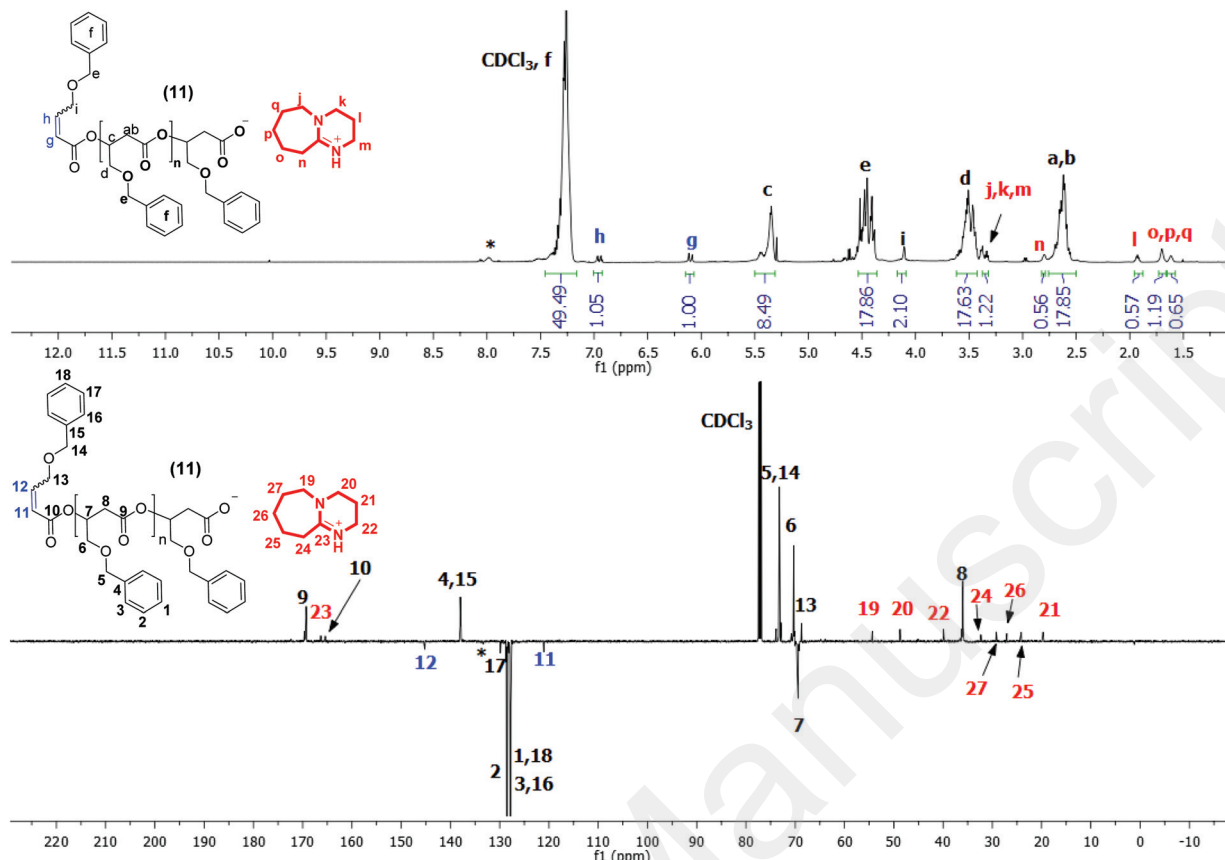


Fig. 7 ^1H (500 MHz, CDCl_3 , 25 $^\circ\text{C}$) (top) and J-MOD (125 MHz, CDCl_3 , 25 $^\circ\text{C}$) (bottom) NMR spectra of PBPL^{OBn} recovered from the ROP of $\text{rac-BPL}^{\text{OBn}}$ mediated by DBU (Table 3, entry 3), depicting only one species (Scheme 4, **11**) out of the two (Scheme 4, **9,11**) (*: unidentified impurity).

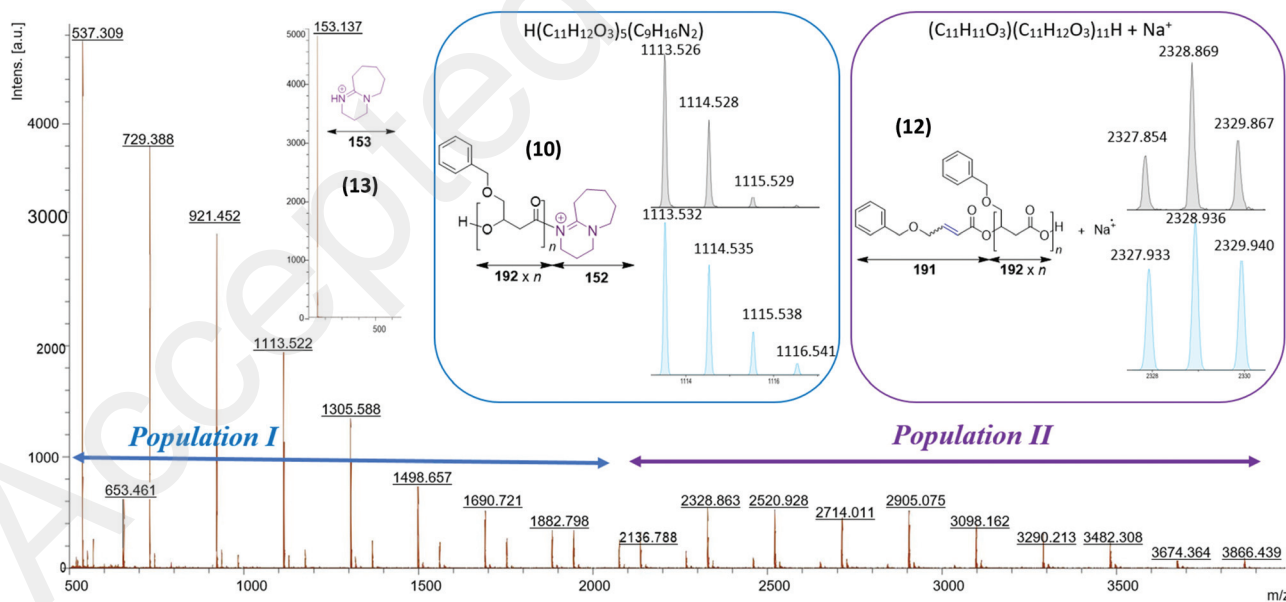
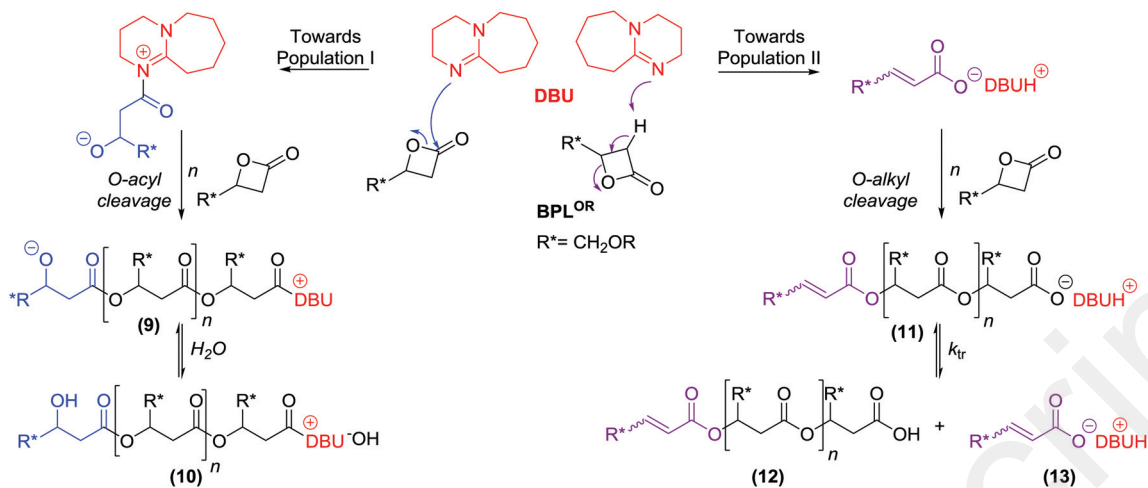


Fig. 8 MALDI-ToF mass spectrum (positive mode, DCTB matrix, Na^+ cationizing agent) of a sample freshly synthesized from the ROP of $\text{rac-BPL}^{\text{OBn}}$ mediated by DBU (Table 3, entry 3) showing populations corresponding to PBPL^{OBn} macromolecules end-capped with both an α -hydroxy and ω -DBU $^+$ groups (population I, Scheme 4, **10**), to PBPL^{OBn} macromolecules ionized with Na^+ and end-capped with both an α -crotonate and ω -carboxylic acid (population II, Scheme 4, **12**), and to DBUH $^+$ (Scheme 4, **13**); the zoomed regions correspond to the simulated (blue, bottom) and experimental (black, top) spectra, respectively. Refer to ESI, Fig. S28† for the MALDI-ToF mass spectrum of same sample analyzed in the absence of a cationizing agent, showing only population I.



Scheme 4 Proposed mechanism for the ROP of *rac*-BPL^{OR} mediated by the dual organocatalyst DBU proceeding either *via* an *O*-acyl cleavage when acting as a nucleophile (blue pathway; **9**), or *via* an *O*-alkyl cleavage when behaving as a base (purple pathway; **11**). Populations I and II observed in the MALDI-ToF mass spectra (Fig. 8) refer to the macromolecular species **10** and **12** obtained upon protonation and transfer reactions, respectively.

The identification of such end-capping groups suggests that DBU behaves as a dual catalyst, both basic and nucleophilic. It would thus mediate the ROP of *rac*-BPL^{OR}s through two competitive mechanistic pathways, in association with the acidic α -H and electrophilic C=O reactivity of BPL^{OR} monomers. Hence, similarly to BEMP, DBU would act as a basic catalyst to form *in situ* the α,β -unsaturated carboxylate-DBU real active species which propagates *via* *O*-alkyl cleavage of the β -lactone to ultimately generate macromolecules of population II (Fig. 8, Scheme 4, **12**). In addition, similarly to TBD, DBU can promote the nucleophilic ROP of *rac*-BPL^{OR}s *via* its *O*-acyl cleavage, generating an alkoxy propagating species to eventually form PBPL^{OBn} corresponding to population I (Fig. 8, Scheme 4, **10**). This latter approach was previously reported for the bulk ROP of lactide using DBU only³² or upon using other amine functional organocatalysis.³³ Further evidence of the DBU's dual activity and of the proposed mechanism was gained from the reinterpretation of the previously reported MALDI-ToF mass spectra of samples recovered from the ROP of MLA^{Bn} mediated by DBU (ESI, Fig. S29†).^{22b}

Conclusion

Functional PHAs, namely PBPL^{OR}s, have been successfully synthesized from the bulk ROP of *rac*-BPL^{OR} monomers at 60 °C using exclusively BEMP, TBD, or DBU as organocatalyst. The activity of these organocatalysts, under these operating conditions, is modest as typically encountered with four-membered ring β -lactones when compared to larger ones (\geq six-membered ring lactones). Their activity towards BPL^{OR}s is lower than in the alike ROP of the related BL and MLA^{Bn} β -lactones; we assume this may be due to the CH₂OR ether substituent which makes the monomer less electrophilic as compared to the methyl or benzyloxycarbonyl function of BL and MLA^{Bn}, respectively.

Inherent to their own intrinsic chemical features, each of the organocatalysts supports a unique mechanistic pathway, as suggested by combined NMR and MALDI-ToF MS detailed analyses of the PBPL^{OR}s. ROP mechanisms at play dictate the nature of the macromolecules' chain-end-groups. BEMP, the most basic and bulky organocatalyst, generates upon proton abstraction and *O*-alkyl cleavage of the BPL^{OR} monomer, a [carboxylate]⁻/[BEMPH]⁺ initiator which propagates the reaction, most likely accompanied by some transfer reactions. BEMP thus appears to behave as a base, similarly to *tert*-butoxide salts that initiate the ROP of BL *via* proton transfer in an irreversible manner.^{29e} On the contrary, the highly nucleophilic TBD forms, *via* *O*-acyl cleavage of BPL^{OR}, a 1:1 *N*-acyl- α,β -unsaturated adduct, that subsequently propagates in the same manner. Finally, the observed dual basic and nucleophilic activity of DBU is comparable to that of the previously reported strong base initiators such as ROK,³⁴ favoring the scission of both *O*-acyl and *O*-alkyl bonds of the BPL^{OR} monomer, eventually forming alkoxy and carboxylate active species, respectively. Apparently, DBU's dual activity prevails once again in the polymerization. The mechanisms proposed herein for the organocatalyzed ROP of BPL^{OR}s mediated by BEMP, TBD or DBU, are fully compatible with those of the alike ROP of BL and MLA^{Bn}, respectively (ESI, Fig. S14, S15, S20, S23 and S29†).²² These results highlight that the mechanism operating in an organocatalyzed ROP of a β -lactone is thus highly dependent on both the chemical nature of the functionality of the monomer's substituent and on the chemical specificity of the organocatalysts used. We assume it may also be strongly affected by the operating conditions used to synthesize the polymers, in particular if the reactions are conducted neat or in solution. We suspect that the latter *modus operandi* parameter might account for the differences observed between Coulembier's work and our studies (refer to the ESI†).²⁴

Conflicts of interest

There are no conflicts to declare.

Acknowledgements

This research was financially supported in part by the Lebanese University and Université de Rennes 1 (Ph.D. grant to R.S.). We are grateful to UMS ScanMAT and especially to Clément Orione and Elsa Caytan, for extensive MS and NMR analyses, respectively.

References

- (a) J. Lu, R. C. Tappel and C. T. Nomura, *Polym. Rev.*, 2009, **49**, 226–248; (b) S. Taguchi, T. Iwata, H. Abe and Y. Doi, *Polymer Science: A Comprehensive Reference*, 2012, vol. 9, pp. 157–182.
- M. Lemoigne, *CR Acad. Sci.*, 1925, **180**, 1539–1541.
- (a) R. W. Lenz and R. H. Marchessault, *Biomacromolecules*, 2005, **6**, 1–8; (b) H. M. Müller and D. Seebach, *Angew. Chem., Int. Ed. Engl.*, 1993, **32**, 477–502.
- (a) B. Laycock, P. Halley, S. Pratt, A. Werker and P. Lant, *Prog. Polym. Sci.*, 2013, **38**, 536–583; (b) K. Sudesh, H. Abe and Y. Doi, *Prog. Polym. Sci.*, 2000, **25**, 1503–1555.
- P. Dubois, O. Coulembier and J.-M. Raquez, *Handbook of Ring-Opening Polymerization*, Wiley-VCH, Weinheim, 2009, pp. 227–254.
- (a) H. R. Kricheldorf and N. Scharnagl, *J. Macromol. Sci., Chem.*, 1989, **26**, 951–968; (b) A. Duda, *J. Polym. Sci., Part A: Polym. Chem.*, 1992, **30**, 21–29; (c) A. Hofman, S. Słomkowski and S. Penczek, *Makromol. Chem.*, 1984, **185**, 91–101.
- For leading reviews on metal-catalyzed ROP of cyclic esters, see: (a) J. F. Carpentier, *Macromol. Rapid Commun.*, 2010, **31**, 1696–1705; (b) C. M. Thomas, *Chem. Soc. Rev.*, 2010, **39**, 165–173; (c) M. J. Stanford and A. P. Dove, *Chem. Soc. Rev.*, 2010, **39**, 486–494; (d) P. J. Dijkstra, H. Du and J. Feijen, *Polym. Chem.*, 2011, **2**, 520–527; (e) S. Dutta, W.-C. Hung, B.-H. Huang and C.-C. Lin, *Synth. Biodegrad. Polym.*, 2011, **245**, 219–283; (f) A. Buchard, C. M. Bakewell, J. Weiner and C. K. Williams, *Top. Organomet. Chem.*, 2012, **39**, 175–224; (g) A. Sauer, A. Kapelski, C. Fliedel, S. Dagorne, M. Kol and J. Okuda, *Dalton Trans.*, 2013, **42**, 9007–9023; (h) S. M. Guillaume, E. Kirillov, Y. Sarazin and J.-F. Carpentier, *Chem. – Eur. J.*, 2015, **21**, 7988–8003; (i) J.-F. Carpentier, *Organometallics*, 2015, **34**, 4175–4189; (j) H. Li, R. Shakahroun, S. M. Guillaume and J.-F. Carpentier, *Chem. – Eur. J.*, 2020, **26**, 128–138.
- N. Ajellal, C. M. Thomas and J.-F. Carpentier, *J. Polym. Sci., Part A: Polym. Chem.*, 2009, **47**, 3177–3189.
- (a) C. G. Jaffredo, Y. Chapurina, S. M. Guillaume and J. F. Carpentier, *Angew. Chem., Int. Ed.*, 2014, **53**, 2687–2691; (b) C. G. Jaffredo, Y. Chapurina, E. Kirillov, J.-F. Carpentier and S. M. Guillaume, *Chem. – Eur. J.*, 2016, **22**, 7629–7641.
- (a) R. Ligny, M. M. Hänninen, S. M. Guillaume and J.-F. Carpentier, *Angew. Chem., Int. Ed.*, 2017, **56**, 10388–10393; (b) R. Ligny, M. M. Hänninen, S. M. Guillaume and J.-F. Carpentier, *Chem. Commun.*, 2018, **54**, 8024–8031; (c) R. Ligny, S. M. Guillaume and J. F. Carpentier, *Chem. – Eur. J.*, 2019, **25**, 6412–6424.
- (a) X. Tang and E. Y.-X. Chen, *Nat. Commun.*, 2018, **9**, 2345; (b) X. Tang, A. H. Westlie, E. M. Watson and E. Y.-X. Chen, *Science*, 2019, **366**, 754–758.
- (a) G. Barouti, K. Jarnouen, S. Cammas-Marion, P. Loyer and S. M. Guillaume, *Polym. Chem.*, 2015, **6**, 5414–5429; (b) G. Barouti, A. Khalil, C. Orione, K. Jarnouen, S. Cammas-Marion, P. Loyer and S. M. Guillaume, *Chem. – Eur. J.*, 2016, **22**, 2819–2830.
- For leading reviews on organocatalyzed ROP of cyclic esters, see: (a) A. Dove, H. Sardon and S. Naumann, *Organic Catalysis for Polymerisation*, Royal Society of Chemistry, 2018; (b) A. Bossion, K. V. Heifferon, L. Meabe, N. Zivic, D. Taton, J. L. Hedrick, T. E. Long and H. Sardon, *Prog. Polym. Sci.*, 2019, **90**, 164–210; (c) W. N. Ottou, H. Sardon, D. Mecerreyes, J. Vignolle and D. Taton, *Prog. Polym. Sci.*, 2016, **56**, 64–115; (d) M. K. Kiesewetter, E. J. Shin, J. L. Hedrick and R. M. Waymouth, *Macromolecules*, 2010, **43**, 2093–2107.
- (a) B. G. G. Lohmeijer, R. C. Pratt, F. Leibfarth, J. W. Logan, D. A. Long, A. P. Dove, F. Nederberg, J. Choi, C. Wade, R. M. Waymouth and J. L. Hedrick, *Macromolecules*, 2006, **39**, 8574–8583; (b) L. Zhang, F. Nederberg, R. C. Pratt, R. M. Waymouth, J. L. Hedrick and C. G. Wade, *Macromolecules*, 2007, **40**, 4154–4158.
- A. Khalil, S. Cammas-Marion and O. Coulembier, *J. Polym. Sci., Part A: Polym. Chem.*, 2019, **57**, 657–672.
- R. Schwesinger, J. Willaredt, H. Schlemper, M. Keller, D. Schmitt and H. Fritz, *Chem. Ber.*, 1994, **127**, 2435–2454.
- (a) Y.-J. Lee, J. Lee, M.-J. Kim, B.-S. Jeong, J.-H. Lee, T.-S. Kim, J. Lee, J.-M. Ku, S.-S. Jew and H.-G. Park, *Org. Lett.*, 2005, **7**, 3207–3209; (b) J. Lee, Y.-I. Lee, M. J. Kang, Y.-J. Lee, B.-S. Jeong, J.-H. Lee, M.-J. Kim, J.-Y. Choi, J.-M. Ku and H.-G. Park, *J. Org. Chem.*, 2005, **70**, 4158–4161.
- (a) D. Simoni, M. Rossi, R. Rondanin, A. Mazzali, R. Baruchello, C. Malagutti, M. Roberti and F. P. Invidiata, *Org. Lett.*, 2000, **2**, 3765–3768; (b) P. Hammar, C. Ghobril, C. Antheaume, A. Wagner, R. Baati and F. Himo, *J. Org. Chem.*, 2010, **75**, 4728–4736; (c) R. Pierre, F. Gaigne, G. El-Bazbouz, G. Mouis, G. Ouvry, L. Tomas and C. S. Harris, *Synlett*, 2018, **29**, 1102–1106.
- (a) H. Oediger and F. Möller, *Angew. Chem., Int. Ed.*, 1967, **6**, 76; (b) H. Oediger, F. Moeller and K. Eiter, *Synthesis*, 1972, 591–598.
- (a) X. Liu, S. Zhang, Q.-W. Song, X.-F. Liu, R. Ma and L.-N. He, *Green Chem.*, 2016, **18**, 2871–2876; (b) J. Sun, W. Cheng, Z. Yang, J. Wang, T. Xu, J. Xin and S. Zhang, *Green Chem.*, 2014, **16**, 3071–3078; (c) J. E. Taylor, S. D. Bull and J. M. Williams, *Chem. Soc. Rev.*, 2012, **41**, 2109–2121;

- (d) R. Reed, R. Réau, F. Dahan and G. Bertrand, *Angew. Chem., Int. Ed. Engl.*, 1993, **32**, 399–401.
- 21 (a) C.-L. Zhang, Z.-F. Zhang, Z.-H. Xia, Y.-F. Han and S. Ye, *J. Org. Chem.*, 2018, **83**, 12507–12513; (b) A. K. Morri, Y. Thummala and V. R. Doddi, *Org. Lett.*, 2015, **17**, 4640–4643; (c) R. Singh, D. S. Raghuvanshi and K. N. Singh, *Org. Lett.*, 2013, **15**, 4202–4205; (d) Y. Thummala, G. V. Karunakar and V. R. Doddi, *Adv. Synth. Catal.*, 2019, **361**, 611–616.
- 22 (a) C. G. Jaffredo, J.-F. Carpentier and S. M. Guillaume, *Macromol. Rapid Commun.*, 2012, **33**, 1938–1944; (b) C. G. Jaffredo, J.-F. Carpentier and S. M. Guillaume, *Polym. Chem.*, 2013, **4**, 3837–3850.
- 23 C. G. Jaffredo, J.-F. Carpentier and S. M. Guillaume, *Macromolecules*, 2013, **46**, 6765–6776.
- 24 S. Moins, C. Henoumont, J. De Winter, A. Khalil, S. Laurent, S. Cammas-Marion and O. Coulembier, *Polym. Chem.*, 2018, **9**, 1840–1847.
- 25 J. A. Schmidt, E. B. Lobkovsky and G. W. Coates, *J. Am. Chem. Soc.*, 2005, **127**, 11426–11435.
- 26 A preliminary set of experiments on the ROP of BPL^{OBn} mediated by BEMP in solution in an NMR tube (C₆D₆, [BPL^{OBn}]₀ = 0.38 mol L⁻¹) showed that the polymerization remained ineffective over 4 h at 60 °C (Conv._{BPL^{OBn}} < 5%), as monitored by ¹H NMR spectroscopy.
- 27 Note that the MALDI-ToF mass spectra previously recorded for PHB and PMLA^{Bn} samples prepared from the alike BEMP mediated ROP of BL and MLA^{Bn}, respectively, could not evidence, the possible presence of –COOH end-capping group because the matrix/cationizing agent used did not enable it.²² A revised analysis of these MALDI-ToF mass spectra is presented in the ESI (ESI, Fig. S14 and S15†) and shows that the ROP of BL and MLA^{Bn} mediated by BEMP proceeds in the same way as the ROP of *rac*-BPL^{ORs}.
- 28 (a) Z. Jedliński, P. Kurcok, M. Kowalczyk and J. Kasperczyk, *Die Makromolekulare Chemie*, 1986, **187**, 1651–1656; (b) O. Coulembier, P. Degée, S. Cammas-Marion, P. Guérin and P. Dubois, *Macromolecules*, 2002, **35**, 9896–9903; (c) G. Y. Adamus and M. Kowalczyk, *Biomacromolecules*, 2008, **9**, 696–703; (d) B. Raeskinen, S. B. Moins, L. Harvey, J. De Winter, C. l. Henoumont, S. Laurent and O. Coulembier, *Macromolecules*, 2019, **52**, 6382–6392.
- 29 (a) Y. Zhang, R. A. Gross and R. W. Lenz, *Macromolecules*, 1990, **23**, 3206–3212; (b) Z. Grobelny, M. Matlengiewicz, K. Skrzeczyna, A. Swinarew, S. Golba, J. Jurek-Suliga, M. Michalak and B. Swinarew, *Int. J. Polym. Anal. Charact.*, 2015, **20**, 457–468; (c) C. Mabile, M. Masure, P. Hémerly and P. Guérin, *Polym. Bull.*, 1998, **40**, 381–387; (d) O. Coulembier, P. Degée, J. L. Hedrick and P. Dubois, *Prog. Polym. Sci.*, 2006, **31**, 723–747; (e) S. Penczek, M. Cypryk, A. Duda, P. Kubisa and S. Słomkowski, *Prog. Polym. Sci.*, 2007, **32**, 247–282.
- 30 (a) S. Kafka, B. Larissegger-Schnell and T. Kappe, *J. Heterocycl. Chem.*, 2004, **41**, 717–721; (b) A. Ying, Z. Li, J. Yang, S. Liu, S. Xu, H. Yan and C. Wu, *J. Org. Chem.*, 2014, **79**, 6510–6516.
- 31 (a) R. C. Pratt, B. G. G. Lohmeijer, D. A. Long, R. M. Waymouth and J. L. Hedrick, *J. Am. Chem. Soc.*, 2006, **128**, 4556–4557; (b) C. Sabot, K. A. Kumar, S. Meunier and C. Mioskowski, *Tetrahedron Lett.*, 2007, **48**, 3863–3866.
- 32 H. A. Brown, A. G. De Crisci, J. L. Hedrick and R. M. Waymouth, *ACS Macro Lett.*, 2012, **1**, 1113–1115.
- 33 (a) V. Katiyar and H. Nanavati, *Polym. Chem.*, 2010, **1**, 1491–1500; (b) H. R. Kricheldorf, N. Lomadze and G. Schwarz, *Macromolecules*, 2008, **41**, 7812–7816.
- 34 Z. Grobelny, S. Golba and J. Jurek-Suliga, *Polym. Bull.*, 2019, **76**, 4951–4966.